

This paper is published in the open archive of Mid Sweden University
DIVA <http://miun.diva-portal.org>
by permission of the publisher

Anatoliy Manuilskiy, Henrik Andersson, Göran Thungström and Hans-Erik Nilsson, "Compact multichannel optical Fourier spectrometer", Proc. SPIE 6395, 639504 (2006);
<http://dx.doi.org/10.1117/12.689653>

© Copyright 2012 Society of Photo-Optical Instrumentation Engineers. One print or electronic copy may be made for personal use only. Systematic electronic or print reproduction and distribution, duplication of any material in this paper for a fee or for commercial purposes, or modification of the content of the paper are prohibited.

Compact Multi Channel Optical Fourier Spectrometer

Anatoliy Manuilskiy¹, Henrik Andersson¹, Göran Thungström¹, Hans-Erik Nilsson¹
¹Mid-Sweden University, Department of Information Technology and Media, SE-851 70 Sundsvall,
Sweden

ABSTRACT

In this work are shown the principle, first experimental results and a model design of a new type of multi channel Fourier transform (FT) spectrometer for visible (VIS) and infrared (IR) region operating in real time. The main principle of this spectrometer is that measured collected and collimated optical radiation passes through a linear array or matrix of optical Fabry-Perot interferometers. Each interferometer is placed in front of and close to each element of the array detector. By processing the signal the spectrum of the optical radiation can be extracted. This design does not require intermediate optics between interferometer and array detector and allows for a reliable and extremely compact construction. Production cost can be low when a simple wedge type interferometer is integrated with existing array or matrix detectors, e.g. CCD camera. One other benefit is that the shape of the interferometer determines whether the spectrometer is suitable for measuring wide spectra radiation or has the ability to discriminate optical coherent radiation. Experimental results achieved for VIS and NIR range of spectra are promising. The principals of this design can be used for a variety of applications besides as a spectrometer. For example warning systems for lasers and restricted coherency sources and also filtering of optical signals and for measuring the spectral content working in a wide spectral range.

Keywords: spectrometer, Fourier transform, IR, laser, laser warning system

1. INTRODUCTION

The use of lasers for range finding equipment, target designators or as guidance for beam riding missiles have made the laser warning receiver (LWR) an important equipment. The LWR must be able to quickly identify laser radiation directed at or near the protected object and to distinguish it from background radiation, such as sunlight. The most common laser radiation for example encountered in military technology are the ruby laser with a wavelength of 0.694 μm , the ND:glass (1.060 μm), ND:YAG (1.064 μm) and the CO₂ laser (10.6 μm). The currently most widely used is the ND:YAG. Usually all lasers encountered in military equipment are pulsed. At the same time development of equipment with continuous wave (CW) lasers makes it necessary for LWRs to be able to detect both pulsed and CW laser radiation. [1-3]. The importance of discriminating radiation from laser sources in laser warning systems was discussed in [3] and it was mentioned that detector selectivity is a more important criterion than detector sensitivity for this applications. For this kind of equipment temporal coherency is one of the properties to distinguish laser radiation. Spatial coherency of the laser can degenerate as it passes through the atmosphere, making it a less suitable parameter to use to discern laser radiation. Some results of development of devices based on arrays of Fabry-Perot etalons or other interferometers exploiting the property of temporal coherency for selecting and imaging laser sources were shown previously [2,3]. Systems with filters and a small number of Fabry-Perot etalon interferometers are often designed in such a way that it only can achieve information about the presence of radiation for a predetermined wavelength range. To overcome this limit an imaging system such as described in [4] could be used, but because it contains interferometer with scanning mirror it can be difficult to operate with pulsed laser radiation. In this work are shown the principle, first experimental results and design of a recently reported kind of multi channel Fourier transform (FT) spectrometer for visible (VIS) and infrared (IR) region operating in real time that does not contain any moving parts and is resistible to mechanical and climatic conditions [5-6]. The design allows to integrate a multi channel interferometer with a detector in one compact spectrometer unit that also have the capability to discriminate both pulsed and CW laser radiation depending on readout electronic design of the array or matrix detector. Such a spectrometer can be used to detect coherent sources as well as extract additional useful information about the spectral content of the radiation. This could be used to implement a LWR based on a multi channel spectrometer with an array of Fabry-Perot interferometers or wedge interferometers attached to an array or matrix detector together with suitable readout electronics and signal processing systems.

2. PRINCIPLE

The main principle of the compact multi channel spectrometer with array or wedge interferometers was described previously in [5,6] and is shown in Fig.1.

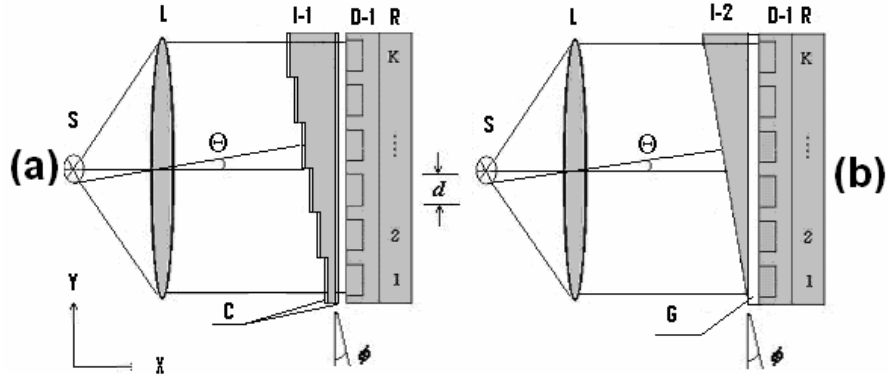


Fig. 1. Optical layouts of the integrated multi channel Fourier spectrometers with stepped (a) and wedge (b) interferometer, S – Optical source, L – Collimated optics, I-1, I-2 – Interferometers, D-1, D-2 – Array detectors with different sized pixels, R – Read out electronics, Θ - Angle of incidence of light, C – Reflection coating, G – Gap between interferometer and detector, ϕ - Wedge angle.

The principle is that measured collected and collimated wide spectra radiation passes through linear array or matrix of the optical Fabry-Perot interferometers with a thickness for example changing linearly, made as optical stepped wedge or wedge. Each interferometer is placed in front of and close to each element of the array detector. By processing the signal the spectrum of the optical radiation can be extracted. This design does not require intermediate optics between interferometer and array detector and allows for a reliable and extremely compact integrated construction. Spectral Response (SR) for an array of Fabry-Perot interferometers with variable thickness of optical pass can be given by

$$h_{\nu,k} = \frac{(1-R)^2}{(1-R)^2 + 4R \left[\sin \left(2\pi \nu W_k \sqrt{n^2 - (n1 \cdot \sin(\Theta))^2} \right) \right]^2} \quad (1)$$

where R – intensity reflectance of each interferometer surface, ν - frequency of incident light (cm^{-1}), n - refraction index of the space surrounding the interferometer, $n1$ - refraction index of the interferometer material, Θ - inclination of incident light and W_k - thickness of interferometer (μm) with number k ($1 \dots k_{\text{max}}$), where k_{max} are determined by highest resolution, and can be defined as (2)

$$W_k = W0 + (k-1)\phi d \quad (2)$$

Where $W0$ - minimal thickness of interferometer (μm), d – distance between interferometer pixels (μm), ϕ - coefficient of thickness change. The intensity of the spectra of the light transmitted by each interferometer is modulated periodically with a spacing of the maximums equal $c/2 \cdot W_k \cdot n1$ where c – speed of light in vacuum ($\mu\text{m/s}$) if angle of the incidence, Θ is small and $n=1$. Spacing is inversely proportional to the optical thickness of the interferometers. It is easy to see from (1) that when R is small the SR is modulated with an even harmonic function of the optical thickness of the interferometers. If the spectral content of the incident light defined by the function $g(\nu)$ then the transmittance of the array of interferometers creates an interference pattern of light intensity behind the array interferometer, which can be defined as (3).

$$I_{\kappa} = \sum_{\nu} h_{\nu,k} g(\nu) \quad (3)$$

The localization of the interference pattern coincides with the interferometer surface if diffraction effects for the used optical layout are not important, interferometer is thin enough and angles of incidence are close to zero [7]. The FT of

intensity of interference pattern gives the spectra of the incident light. Increasing R causes appearance of second and higher harmonics of the spectra. It can be seen from (3) that for non coherent light sources the maximum of the energy of the interference pattern is concentrated when light passes the interferometers with the smallest thickness and this part of the interferometer is important for analyses of such kind of light. The thicker part of the interferometer is important for analysis of light with higher coherency. The requirements to obtain a correct spectrum after FT is that the interferometer array should contain individual interferometers with thickness range from zero to chosen maximum thickness and with a step of optical thickness less than half of the shortest wavelength in incident radiation. Just a wedge (not stepped) shaped interferometer can be used if the wedge angle, φ , is so small that the period of the interference pattern for the shortest wavelength of interest is at least two times greater than the distance between array pixels, Fig. 1b. For a small reflection coefficient, R, a wedge shaped interferometer produces interference patterns similar to interference patterns created by two beams inclined on a small angle, 2φ . At the same time according to the optical layout, Fig. 1, it is impossible to achieve phase shift between interfering beams from negative – trough zero – to positive values which usually are used in standard FT spectrometers with Michelson interferometers. The last one can produce two sides interferogram for the spectrum reconstruction. If the phase change start from zero it can be used so called Fourier Cosine expansion, [8], to construct two sides from one side interferogram. In practice it is not easy to reach initial zero phase difference when using a wedge interferometer because of manufacturing limitations. As a result some wedge interferometers, hereafter called "restricted wedge", produces an interferogram with missing information for small phase shifts. As mentioned previously the missing information for small phase shifts leads to suppression of spectral components with low coherency. At the same time for the partially coherent and coherent light using a restricted wedge is not a limiting factor for spectra reconstruction. Restricted array Fabry Perot or wedge interferometer with a non zero minimal thickness creates a interference pattern which can be considered as windowed interferogram. Spectrum of the windowed interferogram can be achieved by the Fourier transform of the product of the functions representing the window and intensity of the interferogram. Fourier transform of this product can be also performed as convolution of the spectra of the above mentioned functions. Let us assume that the incident light is a planar wave. Behind the wedge interferometer there are two planar waves inclined by angle $2 \cdot \varphi$ shown in Fig.2a. and

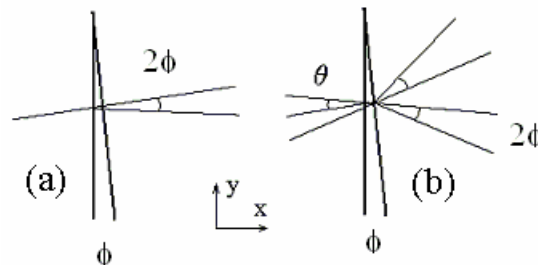


Fig. 2. Thin optical wedge: illustrating of formation of waves.

for each incident monochromatic wave of the frequency ν it creates periodical interference pattern of the intensity with

$$\text{spatial frequencies } \xi = \frac{2 \cdot \nu \cdot \varphi \cdot n}{c} \quad (4)$$

Assume that the spectral content of the incident optical beam and therefore the spatial spectrum of the interferogram can be described by a Gaussian distribution with a frequency of the maximum - ξ_0 and given by

$$S_{\xi} = e^{-\ln(2) \left(\frac{\xi - \xi_0}{\Delta s} \right)^2} \quad (5)$$

where Δs – half width of the spatial spectra .

The window function can be written as

$$W_y = e^{-\ln(2) \left(\frac{y - y_0}{a} \right)^2} \quad (6)$$

where a - half width and y_0 - offset of the window function. The normalized spatial spectrum of the window function taking into account the shift or offset of the center of the window from the beginning of the interferogram by y_0 can be written as

$$SWf(\xi_j) = e^{-2\pi i \xi_j y_0} e^{-\ln(2) \left(\frac{\xi_j}{\Delta w} \right)^2} \quad (7)$$

Where $\Delta w = \frac{2 \cdot \sqrt{\ln(2)}}{\pi \cdot a}$ is a half width of the spatial spectra of window function

The resulting amplitude of the spectrum of the windowed interferogram can be written in the form

$$WSPf(\xi) = \frac{1}{\Delta w} \int_0^{\xi_{\max}} e^{-\ln(2) \left(\frac{\xi_j - \xi_0}{\Delta s} \right)^2} e^{-2\pi i (\xi_j - \xi) y_0} e^{-\ln(2) \left(\frac{\xi_j - \xi}{\Delta w} \right)^2} d\xi_j \quad (8)$$

This can be simplified as

$$WSPf(\xi) = e^{-\frac{\ln(2) \cdot (\xi - \xi_0)^2}{(\Delta w^2 + \Delta s^2)} \beta_{\max}} \int_0^{\beta_{\max}} e^{-2\pi i (\beta) y_0} e^{-\ln(2) \left(\frac{\Delta w^2 + \Delta s^2}{\Delta w^2 \cdot \Delta s^2} \right) (\beta - \beta_1)^2} d\beta \quad (9)$$

where $\beta = \xi_j - \xi$ and $\beta_1 = \frac{\Delta w^2 (\xi_j - \xi)}{\Delta w^2 + \Delta s^2}$.

For the reasonable spectral resolution of the spectrometer Δw and window offset X_0 the integral in (9) strongly depends on Δs and approximately equal to

$$A(\Delta s, \Delta w, y_0) = e^{-\frac{(\pi \cdot y_0)^2 \cdot \left(\frac{\Delta w^2 \cdot \Delta s^2}{\Delta w^2 + \Delta s^2} \right)}{\Delta w^2 + \Delta s^2}} \quad (10)$$

and (9) can be rewritten as.

$$WSPf(\xi) \approx e^{-\frac{(\pi \cdot y_0)^2 \cdot \left(\frac{\Delta w^2 \cdot \Delta s^2}{\Delta w^2 + \Delta s^2} \right)}{\Delta w^2 + \Delta s^2}} \cdot \frac{\ln(2) \cdot (\xi - \xi_0)^2}{(\Delta w^2 + \Delta s^2)} \quad (11)$$

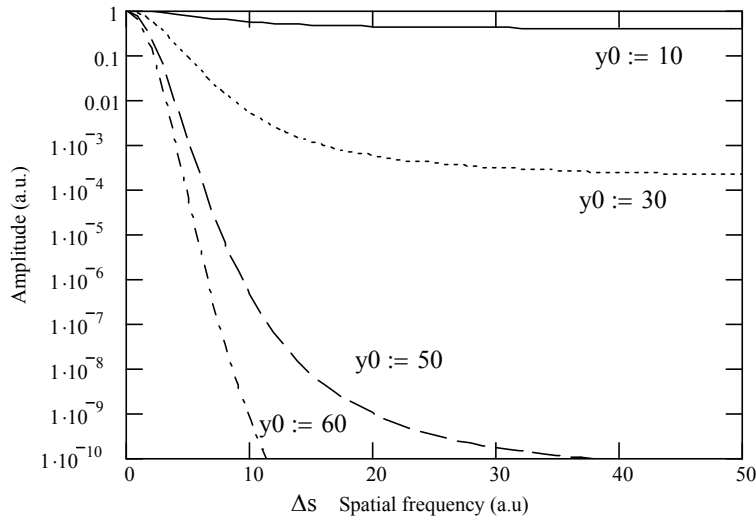


Fig. 3. Dependence of response of the spectrometer with restricted wedge on level of coherency.

The second term of the right side of (11) describes the gaussian shape of the reconstructed spatial spectrum with half width $\Delta w^2 + \Delta s^2$ and the first term corresponds to the amplitude of the spectrometer response to radiation of different coherency. Fig.3 represents the dependence of the amplitude A as a function of Δs expressed by (10) and parameter y_0 .

Achieved data is calculated for interferogram containing 256 pixels and $\Delta_w=8$. The simulation and of the spectral response of a spectrometer with a restricted wedge interferometer were also done for the case when incident light contains a mixture of strong partially coherent and weak coherent light with a Gaussian spectra of width 100 nm and 1 nm respectively. The alternative part of the distribution of the intensity of the incident light in the Y direction and the signal from the array detector attached to interferometer can be written as a sum of all the spectral components

$$I_y = \sum_{\xi} \cos(2\pi \cdot \xi \cdot y) \cdot e^{-\left(\frac{\xi-\xi_0}{\Delta_1}\right)^2} + \sum_{\xi} \cos(2\pi \cdot \xi \cdot y) \cdot e^{-\left(\frac{\xi-\xi_0}{\Delta_2}\right)^2} \quad (12)$$

where the first and the second terms is the contribution of the low and high coherency sources. Coherency of the waves are determined by parameters Δ_1 and Δ_2 . If the thickness of the interferometer varies from w_0 to w_{max} the interference pattern will correspond to one side interferogram and after Cosine expansion it can be used for Fourier reconstruction of the spectrum of the incident light. The window or apodization function was similar to (6). The spectrum of the incident light is shown in Fig. 4a. In this case the wedge interferometer produces the one side interferogram shown in Fig. 4b (solid line), which was used for reconstruction of the spectra of the incident light. If the window function is applied to the interferogram as shown by the dotted line in Fig. 4b, then the resulting spectrum achieved by the spectrometer is shown in Fig. 5. It can be seen that the ratio of intensities for the obtained response for coherent and partially coherent radiation is of the order 40dB. Such selectivity of the response of the spectrometer with a restricted wedge interferometer can be qualitatively explained if take into account the difference between amplitude and phase structure of the Fourier spectra of the window function centered and shifted from the center of the interference pattern in Fig. 4. The phase

oscillations with amplitude $\pm \pi/2$ in the shifted window spectra according to (7) results in a decreasing amplitude when convolution is done of the spectrum of non or partially coherent radiation and the spectrum of the shifted window function.

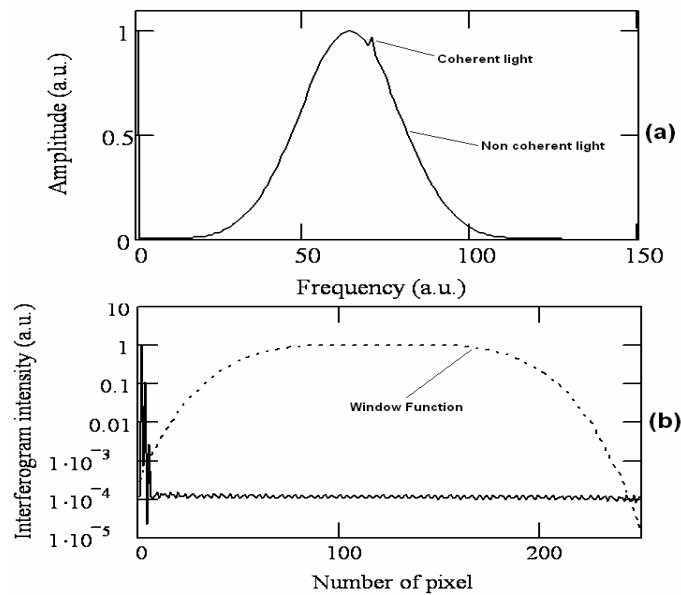


Fig. 4. Spectrum of incident light containing non coherent and weak coherent components, (a), and corresponding interferogram, intensity vs. number of pixels (solid line) and window function (dotted line), (b).

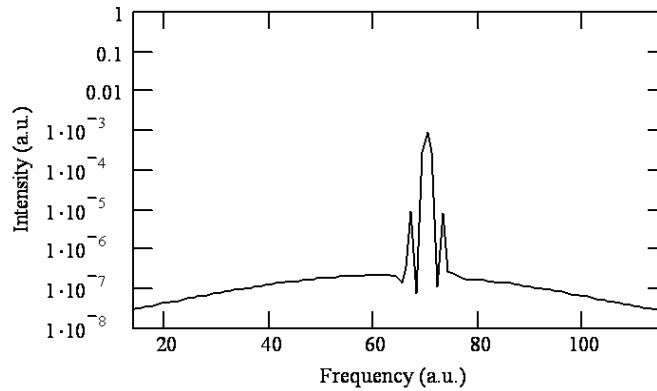


Fig. 5. Resulting spectrum achieved by MCFTS with restricted wedge is the convolution of the window function and the incident light spectra.

3. RESULTS

The setup for characterization of previously described types of compact FT spectrometers consists of a wedge shaped interferometer with an air gap between interferometer mirrors for the first experiments, see Fig. 6. Interferometer material with higher refractive index, for

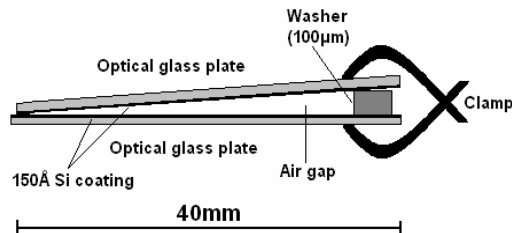


Fig. 6. Wedge shaped interferometer with air gaps between interferometer mirrors.

example Si, can be more effective to use because it does not require additional coating of the surfaces. Interferometer mirrors with suitable reflection and transmission were manufactured with glass plates coated with 150Å Si layer to produce a wedge shaped air gap interferometer. The mirrors were coated with a Si layer because it is much more resistible to wear when in mechanical contact then for example Al. Measured reflectance for Si coated mirrors for a wide spectral range is shown in Fig. 7. For a wedge interferometer with angle $\varphi = 2$ mrad and length 50mm the interferometer mirrors were separated from one side with a washer made from a 100 μm thick Si wafer and squeezed by a clamp in such a way that opposite sides of the mirrors had a very small gap, Fig.6. The quality of the interferometer which depends on the linearity of the changing thickness of the air gap was checked by obtaining Fourier spectra of 630nm and

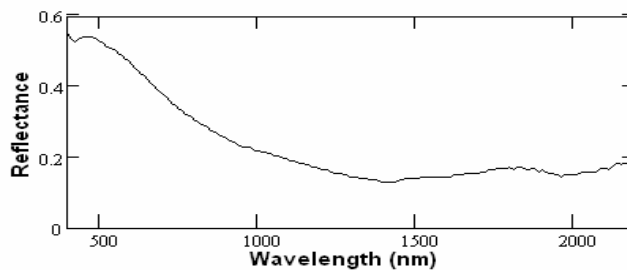


Fig. 7. Measured reflectance for Si coated mirrors for a wide spectral range.

was also checked by taking interferograms from coherent optical sources with different wavelengths. These interferometers were attached to different kinds of array and matrix detectors to assemble spectrometers. The detectors used were a Xenics 256 pixel extended InGaAs array working up to 2.5 μm , a Hamamatsu 1024 pixel Si array and a 320x240 pixel standard Si matrix detector. Different laser and LED sources were used to characterize the spectrometers. For laser sources no optics was used between the laser and wedge interferometer. For experiments with partially coherent radiation optics were used to collect light from the reflectance standard. Fig.8a shows the spectra obtained from a 630nm and a 1560nm laser source simultaneously. Fig.8b shows the spectra of a 630nm laser and a 940nm LED source obtained simultaneously.

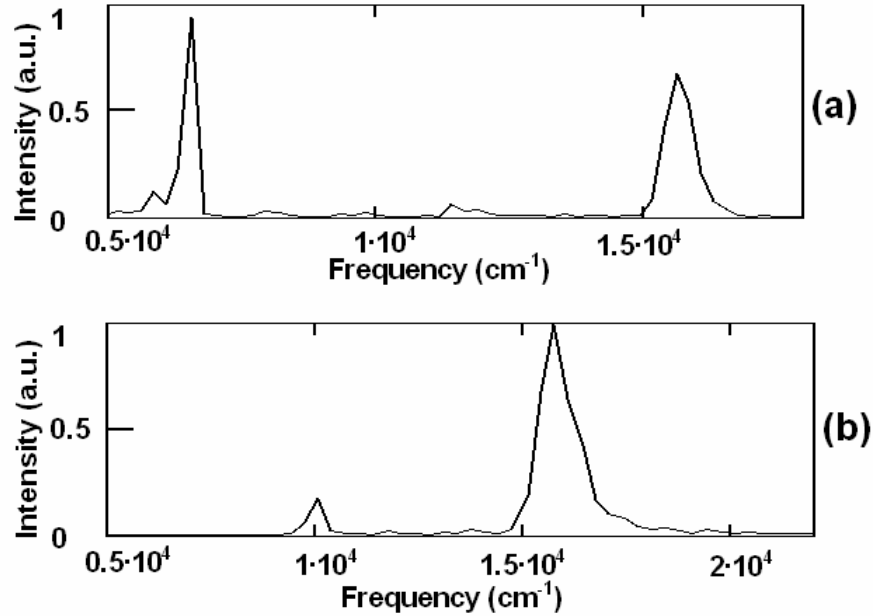


Fig. 8. Spectra obtained from a 630nm and a 1560nm laser source simultaneously, (a) and spectra of a 630nm laser and a 940nm LED source obtained simultaneously, (b).

4. DISCUSSION

It was shown previously that simple compact FT spectrometers equipped with an array or matrix detector attached to a thin restricted wedge interferometer is effective for distinguishing the presence of coherent radiation. For practical applications it is possible to use commercially available array detectors and combine them with a manufactured wedge interferometer into a spectrometer system with selectivity for coherent laser and partially coherent radiation. Although most commercial detectors have a window covering the detector making it impossible to attach the interferometer wedge without leaving a gap between. This gap limits the performance of such kind of spectrometers and therefore a simulation was done to describe the influence of the gap distance. Simulations were done to estimate the tolerance on the distance from the interferometer to the detector when the spectral content of the incident wave can still be measured with an appropriate spectral resolution. In the simplest case each incident optical planar wave propagates through the wedge interferometer, which is constructed by placing two inclined reflecting surfaces as shown in Fig.1a. If the angle of the incidence is equal to θ and taken in to account only one reflection inside of the interferometer then the alternative (time independent) part of the amplitude of the wave after interferometer can be described as a composition of two inclined planar waves propagating with the angles $\pm \theta$. A wave from the extended source can be described as a sum of planar waves from incoherent sources with a wave vectors within the cone $\pm \theta$. If the wedge angle φ is small the convergence of the incident light can be considered within the cone of angle 2θ . For this case the intensity of the interference pattern created by the interferometer on the distance x from interferometer can be written as

$$a_{x,y} = \sum_{\nu} \sum_{\theta} \frac{1}{(\varphi \max + 1) \cdot (\nu \max + 1)} \cdot \cos[4 \cdot \pi \cdot \nu \cdot y \cdot \cos(\theta) \cdot \sin(\varphi)] \cdot \cos[4 \cdot \pi \cdot \nu \cdot x \cdot \sin(\theta) \cdot \sin(\varphi)] \quad (13)$$

The plots in Fig.9-12 show the dependence of the contrast of the interference pattern vs. the distance to the detector based on calculations with (13). The changes of the divergence of the incident light in this simulation are in the range 10-150 mRad. Fig.9 and Fig.10 corresponds to the case when incident light is monochromatic with frequency 10^4 cm^{-1} and Fig.11 and Fig.12 non coherent with spectral range from $8000\text{-}12000 \text{ cm}^{-1}$. Fig. 9 and Fig. 11 shows the results of simulation using eq.13 using parameters $\varphi=5\text{mRad}$ that corresponds to required maximal pixel size for the detector, $50\mu\text{m}$. For Fig.10 and Fig.12 the parameter $\varphi=25\text{mRad}$ that corresponds to maximal pixel size for the detector $10\mu\text{m}$. For coherent and non coherent radiation with reasonable acceptance angle $\theta = 100\text{mRad}$ and the contrast of the interferogram equal 0.5 the distance to the detector with pixel size 50 and $10\mu\text{m}$ equals approximately $300\mu\text{m}$ and $60\mu\text{m}$ respectively. A larger distance between detector and interferometer is allowed for smaller acceptance angles. In Fig.8 is shown the experimental results achieved with a commercial InGaAs detector array (Xeva type) made by Xenics. As many detectors it has a cover window that allows a minimal accessible distance between interferometer and detector, in this case about 3mm. As shown by simulation reasonable results can be achieved with coherent sources like lasers, see Fig. 9-10. Another limiting factor for acceptance angle can be derived from eq.1. It can be seen that the limiting acceptance angle is a function of thickness of the interferometer and it shows that thicker wedge interferometers requires smaller acceptance angles when high spectral resolution is required. Optimal maximal thickness of the interferometer can be estimated by trading resolution and acceptance angle.

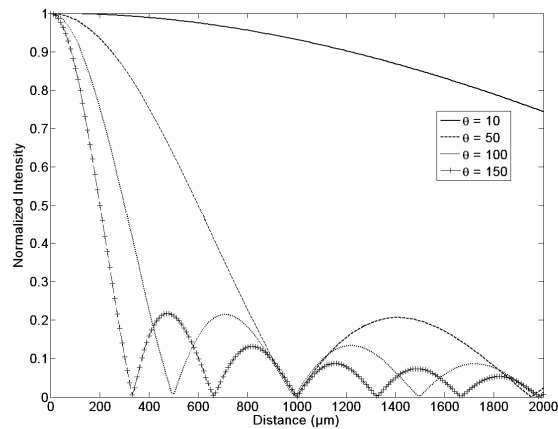


Fig. 9. Dependence of the contrast of the interference pattern vs. the distance to the detector: for coherent radiation and interferometer inclination angle $\varphi=5\text{mRad}$.

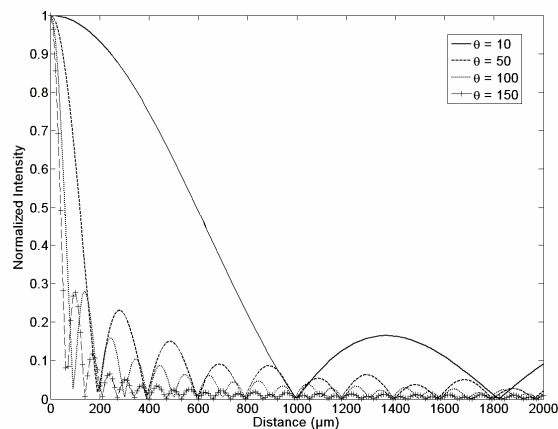


Fig. 10. Dependence of the contrast of the interference pattern vs. the distance to the detector: for coherent radiation and interferometer inclination angle $\varphi=25\text{mRad}$.

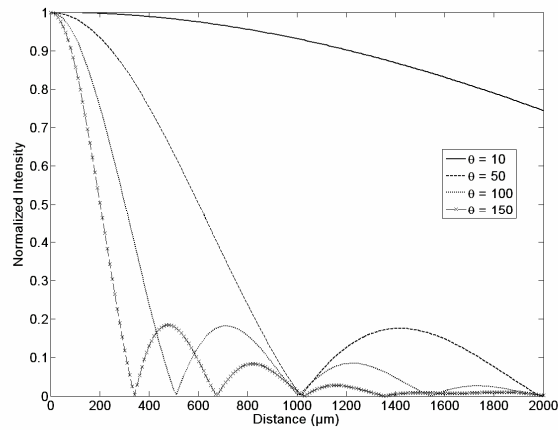


Fig. 11. Dependence of the contrast of the interference pattern vs. the distance to the detector: for non coherent radiation and interferometer inclination angle $\varphi=5\text{mRad}$.

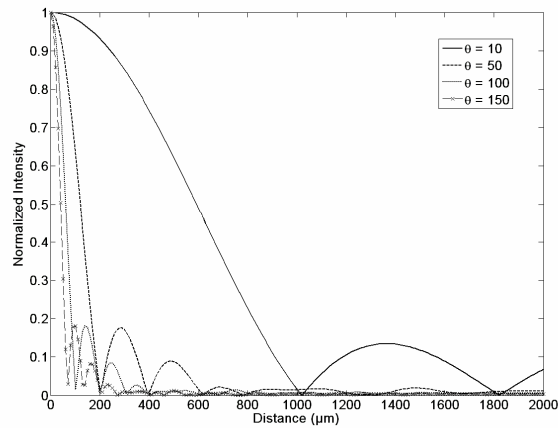


Fig. 12. Dependence of the contrast of the interference pattern vs. the distance to the detector: for non coherent radiation and interferometer inclination angle $\varphi=25\text{mRad}$.

5. CONCLUSION

According to simulations and measurements presented here Multi Channel Fourier Transform Spectrometer can be used for discriminating radiation of such coherent sources as gas and solid state pulsed and CW lasers, as well as partially coherent sources as LED. Reasonable acceptance angle about 100 mRad with wedge interferometer of thickness from tenth to a few hundreds microns respectively attached to commercial array or matrix detectors can be achieved. The ratio of intensities for the obtained response for coherent and partially coherent radiation is of the order 40dB. Simplicity of the multi channel FTS with a wedge shaped interferometer makes it attractive for many applications as for example warning laser systems. This principle of the compact multi channel Fourier spectrometer can be used in the different spectral ranges from UV to Far Infrared.

REFERENCES

1. P.A. Forrester and K.F. Hulme, "Review Laser rangefinders", *Opt. and quantum electronics*, 13, 259-293 (1981)
2. J. Pietzak, "Laser warning receivers", *Laser Technology VII: Applications of lasers, Proceedings of SPIE Vol. 5229* (2003)D.H. Pollock, "*The Infrared & Electro-Optical Systems Handbook Vol.7 Countermeasure Systems*", SPIE Optical Engineering Press, 1993, ISBN 0-8194-1072-1
3. V.A. Manasson and L.S. Sadovnik, "Laser Warning Receiver Based on Coherence Discrimination" Aerospace and Electronics Conference, 1996. NAECON 1996., Proceedings of the IEEE 1996 National
4. C.J. Duffy and D. Hickman, "An Imaging System Based On Temporal Coherence Differences", *J.Phys, D: Appl. Phys*, 21, S56-S58, (1988)
5. Guerineau et al. "Stationary Fourier Transform Spectrometer" U.S. Patent 2004/0239939 A1, Dec. 2, 2004
6. A. Manuilskiy et al., "Multi Channel Array Interferometer-Fourier Spectrometer", to be published
7. M. Born, E. Wolf, "Principles Of Optics", Cambridge University Press, 1999, ISBN 0521642221
8. A. Jeffrey, "Mathematics for Engineers and Scientists", Chapman & Hall, 1989, ISBN 0-412-44540-9